Springer

Dear Author:

Please find attached the final pdf file of your contribution, which can be viewed using the Acrobat Reader, version 3.0 or higher. We would kindly like to draw your attention to the fact that copyright law is also valid for electronic products. This means especially that:

- You may not alter the pdf file, as changes to the published contribution are prohibited by copyright law.

- You may print the file and distribute it amongst your colleagues in the scientific community for scientific and/or personal use.

- You may make an article published by Springer-Verlag available on your personal home page provided the source of the published article is cited and Springer-Verlag is mentioned as copyright holder. You are requested to create a link to the published article in LINK, Springer's internet service. The link must be accompanied by the following text: The original publication is available on LINK **http://link.springer.de.** Please use the appropriate URL and/or DOI for the article in LINK. Articles disseminated via LINK are indexed, abstracted and referenced by many abstracting and information services, bibliographic networks, subscription agencies, library networks and consortia.

- You are not allowed to make the pdf file accessible to the general public, e.g. your institute/your company is not allowed to place this file on its homepage.

- Please address any queries to the production editor of the journal in question, giving your name, the journal title, volume and first page number.

Yours sincerely,

Springer-Verlag Berlin Heidelberg

Ocean Dynamics (2001) 52: 58–70
DOI 10.1007/s10236-001-0007-y

Katja Fennel

The generation of phytoplankton patchiness by mesoscale current patterns

Received: 31 March 2001 / Accepted: 31 August 2001

Abstract Elken et al. (1994) suggested that phytoplankton patchiness can be generated by mesoscale eddies in light-limited, nutrient-replete environments. This hypothesis is explored using two ecological models of different physical complexity. The model results support the idea that the coupling of mesoscale eddy circulation and phytoplankton growth leads to differential growth rates and thus generates variability in phytoplankton distributions. The specific circulation of a cyclonic eddy isolates a phytoplankton population in its core. Due to the reduced vertical mixing, a higher growth rate is supported in the core, and phytoplankton concentrations increase compared to the surrounding environment. A one-dimensional model is used to explore the hypothesis in general and to perform sensitivity studies. A more realistic simulation uses a coupled three-dimensional model for the western Baltic Sea. Starting from vertically and horizontally homogeneous distributions for nutrients and plankton, the models generate patchiness due to the proposed mechanism. The described mechanism may apply for other mesoscale variable environments during light-limited growth periods as well, e.g., the frontal region of the Southern Ocean.

Keywords Phytoplankton patchiness · Mesoscale eddy · Coupled model · Spring bloom · Baltic Sea

Responsible Editor: Roger Proctor

K. Fennel
Baltic Sea Research Institute,
Warnemünde, Germany

Present address:
Oregon State University,
COAS, 104 Ocean Admin. Bldg.,
Corvallis, OR 97331, USA
e-mail: kfennel@coas.oregonstate.edu

1 Introduction

The distribution of marine organisms is generally not uniform over space. A considerable degree of spatial heterogeneity is present at most trophic levels and most spatial scales (Denman and Platt 1976; Mackas et al. 1985; Abbott and Zion 1987; Davis et al. 1992; Kononen et al. 1992; Steele and Henderson 1992; Abbott and Barksdale 1995; Siegel et al. 1999). This patchiness in plankton distributions is surprising in view of the homogenizing effect of diffusion and mixing, which tend to decrease spatial gradients. There must be powerful mechanisms, able to induce spatial gradients in plankton distributions against the homogenizing physical mixing processes. Different explanations have been suggested for the generation of these heterogeneous plankton distribution patterns. For example, studies by Levin and Segel (1976), Mackas and Boyd (1979), Steele and Henderson (1992), Powell and Okubo (1994), Solow and Steele (1995) have focused on predator–prey interactions to explain plankton patchiness, while Gower et al. (1980), Aitsam (1994), Malchow (1994), Smith et al. (1996), Abraham (1998) have suggested different physical mechanisms.

In the Baltic Sea a considerable degree of phytoplankton patchiness is observed during early spring prior to the start of the spring bloom. The phytoplankton patches are closely associated with mesoscale current features such as fronts, jets, and eddies (Kononen et al. 1992; Siegel et al. 1999). Phytoplankton growth in the Baltic Sea is generally assumed to require thermal stratification; however, localized phytoplankton patches are observed prior to the establishment of the thermocline. The emergence of these local phytoplankton maxima is intriguing, since growth conditions are homogeneous in terms of nutrient supply and grazing pressure at this time of the year. Patchiness generation mechanisms such as spatially restricted upwelling of nutrients (Aitsam 1994) or patterns in grazing pressure (Steele and Henderson 1992) can be excluded as possible explanations, since nutrients are available in saturated

concentrations in early spring and are distributed homogeneously due to the deep vertical mixing in late winter (Nehring et al. 1995, 1996; Matthäus et al. 1997). Zooplankton abundances are very low at this time of the year (HELCOM 1996).

Elken et al. (1994) proposed a generation mechanism that arises from the nonlinear response of phytoplankton growth to the ocean current field. The authors suggest that mesoscale eddies increase phytoplankton growth locally, since their specific circulation isolates distinct water masses. In cyclonic eddies the core is isolated, and vertical mixing is reduced in the center, while vertical mixing is enhanced in the region surrounding the eddy core (Onken 1990). Since the depth of the vertical mixing is a crucial factor for phytoplankton growth in early spring, when the phytoplankton community is limited by light (Sverdrup 1953), growth can be enhanced locally in the eddy core compared to the deeply mixed area surrounding the eddy core and the moderately mixed ambient environment. This mechanism does not require the existence of a thermocline and can occur prior to the establishment of thermal stratification, which is generally regarded as a necessary prerequisite for phytoplankton growth in the Baltic Sea.

A significant impact of mesoscale eddies on phytoplankton productivity has been recognized in other regions of the world's oceans as well, including the Southern Ocean and the North Atlantic Ocean. In the high-nutrient, low-chlorophyll environment of the Southern Ocean the mesoscale-active parts of the Antarctic Circumpolar Current (ACC) stand out as regions of high chlorophyll (Strass et al. 1998; Moore et al. 1999). Since macronutrients are replete and light limitation is important in the Southern Ocean (Nelson and Smith 1991), this environment is comparable to the early spring situation in the Baltic Sea. Eddy dynamics also influence primary productivity in the oligotrophic Sargasso Sea in the North Atlantic (Falkowski et al. 1991; McGillicuddy et al. 1998; Oschlies and Garçon 1998). The uplifting of the water column in the center of cyclonic eddies transports nutrients upward. Since phytoplankton growth is nutrient-limited in this region, the nutrient input into the euphotic zone stimulates phytoplankton growth.

This study is intended to corroborate the proposed hypothesis that differences in the magnitude of vertical mixing associated with the mesoscale current field are able to generate phytoplankton patchiness. A simple biological model combined with two physical frameworks of different complexity is used to raise evidence. A process-oriented model, which resolves only vertical processes and does not relate to specific topographical or forcing conditions, is implemented to explore the hypothesis in general. The results show that the proposed mechanism leads to spatial patterns in phytoplankton growth during the first 2 weeks of the bloom and quickly produces horizontal gradients. Because of its simplicity, the model allows one to analyze the balance of the phytoplankton sources and sinks and the sensitivity of the model results to choices of parameterizations and single parameters.

A three-dimensional coupled physical/biological simulation captures a more realistic picture of the processes in the western Baltic Sea. The model resolves the mesoscale dynamics of nutrients and plankton in response to realistic external forcing during spring. A high degree of patchiness evolves which corresponds qualitatively to observed patterns of phytoplankton patchiness. The effect of one mesoscale eddy is discussed as an example to show that the simulated patchiness can be explained by the proposed mechanism.

2 Model description

2.1 The biological model

The biological model employed in this study is a relatively simple representation of the nitrogen cycle mainly conceived to describe the dynamics of nutrients and phytoplankton in the water column (Fig. 1). It is based on the model of W. Fennel (1995) and comprises the four state variables: limiting nutrient N, phytoplankton P, zooplankton Z, and detritus D. The growth rate of phytoplankton w is determined by a modified Michaelis-Menten function in combination with Steele's (1962) parameterization of the photosynthetically active radiation

$$w(N,I) = w_{\max}\frac{N^2}{k_N + N^2}\frac{I}{I_{\text{opt}}}\exp\left(1 - \frac{I}{I_{\text{opt}}}\right) \quad . \tag{1}$$

I is the incident solar radiation while I_{opt} is an assumed optimal radiation value for photosynthesis. I_{opt} is set to a quarter of the incoming radiation just below the surface, but does not drop below a value of 25 W m^{-2} following Stigebrandt and Wulff (1987). The parameters $w_{\max}$ and k_N represent the maximum growth rate and the half-saturation concentration for nutrient uptake, respectively. Phytoplankton loss terms comprise grazing by zooplankton, linear metabolical losses due to respiration (L_{PN}), and mortality (L_{PD}) and sinking. The

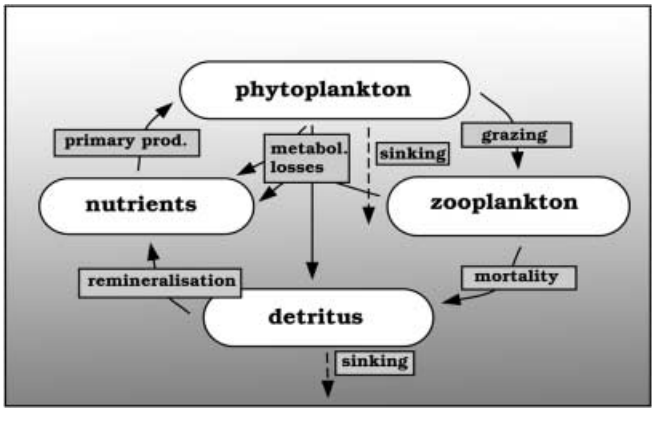

Fig. 1 Scheme of the chemical-biological model

zooplankton grazing g is determined by the modified Ivlev function

$$g(P) = g_{\max}\left[1 - \exp(-I_v P^2)\right] \ , \tag{2}$$

where $g_{\max}$ is the maximum grazing rate and I_v is the Ivlev constant. The zooplankton loss term L_Z comprises the linear mortality and exudation rates L_{ZD} and L_{ZN}. Dead particles are assumed to sink at a constant rate w_D of 5 m day^{-1}. As suggested by Stigebrandt and Wulff (1987), a variable sinking velocity w_P is assumed for phytoplankton, that reads

$$w_P = w^\circ P^2 \ , \tag{3}$$

where w° is a constant factor. Sunken particles accumulate in the bottom layer and are subject to remineralization there. A benthic layer and benthic processes are not included explicitly. The biological sources minus sink terms (sms) read explicitly

$$\begin{aligned}\mathrm{sms}(N) = &-w(I,N)P + L_{PN}(P - P_0) \\ &+ L_{ZN}(Z - Z_0) + L_D D\end{aligned} \tag{4}$$

$$\mathrm{sms}(P) = -w_P \frac{\partial P}{\partial z} + w(I,N)P - g(P)Z - L_P(P - P_0) \tag{5}$$

$$\mathrm{sms}(Z) = g(P)Z - L_Z(Z - Z_0) \tag{6}$$

$$\begin{aligned}\mathrm{sms}(D) = &-w_D \frac{\partial D}{\partial z} + L_{PD}(P - P_0) \\ &+ L_{ZD}(Z - Z_0) - L_D D.\end{aligned} \tag{7}$$

The employed parameter values are given in Table 1. Small background values P_0 and Z_0 are included in the linear loss rates of phytoplankton P and zooplankton Z. This has been found to be important if the model is run over seasonal cycles to ensure that plankton do not go extinct during the nongrowing season and that seed populations are always present.

2.2 A process-oriented vertical model

A process-oriented model was implemented by defining a simple physical frame for the biological model. Only vertical processes are taken into account; that is, vertical mixing of the biological variables and sinking of phytoplankton and detritus. The model is set up on a longitudinal slab of 50 km length and 50 m depth. The horizontal grid width is 0.5 km and the vertical resolution is 0.5 m. A sine shape of the mixed layer depth is assumed to resemble the variation of vertical mixing associated with a cyclonic eddy (Fig. 2). The mixing coefficients are set to 50 cm^2 s^{-1} and 0.05 cm^2 s^{-1} in the mixed layer and below the mixed layer, respectively. The mixed layer depth mld is defined as

$$\mathrm{mld}(x) = c_1 \sin\left(\frac{3\pi x}{x_{\max}}\right) + c_2 \ , \tag{8}$$

where $x \in [0, x_{\max}]$ is the longitudinal coordinate, $c_2 = 20$ m represents the mean mixed layer depth, and $c_1 = 10$ m is the size of the fluctuations from the mean depth.

The daily cycle of incoming solar radiation is calculated according to the astronomical formula (Brock 1981) assuming a constant cloudiness of 3 oktas. The effect of cloud cover is parameterized according to Smith and Dobson (1984). The initial conditions for the simulation correspond to the typical conditions in early spring in the Arkona Sea (western Baltic Sea) and agree with the initial conditions for the three-dimensional simulation described later on. The initial nutrient

Table 1 Parameter values of the chemical-biological model

Symbol	Definition	Value
$w_{\max}$	Maximum growth rate	1.0 day^{-1}
$w_{\max_0}$	Maximum growth rate at 0 °C	0.8 day^{-1}
$I_{\mathrm{opt}} = \max(0.25I_0, I_{\min})$	Optimal radiation	
$I_{\min}$	Minimum of optimal radiation	25 W m^{-2}
$P^B_{\max}$	Maximum rate of photosynthesis (Eq. 12)	4
α	Initial slope of the light response(Eq. 12)	0.02 (W m^{-2})$^{-1}$
a	Exponent in $w_{\max}(T)$, $L_{PN}(T)$, and $L_D(T)$	0.063 °C^{-1}
k_N	Half saturation coefficient of nutrient uptake	0.09 mmol^2 m^{-6}
$g_{\max}$	Maximum grazing rate	0.5 day^{-1}
I_v	Ivlev coefficient	1.1 (mmol N)$^{-2}$ m^6
L_{PN}	Exudation rate	0.08 day^{-1}
e_0	Exudation rate at 0 °C	0.06 day^{-1}
L_{PD}	Mortality rate of phytoplankton	0.02 day^{-1}
$L_P = L_{PN} + L_{PD}$		
L_{ZN}	Respiration rate of zooplankton	0.01 day^{-1}
L_{ZD}	Mortality rate of zooplankton	0.02 day^{-1}
$L_Z = L_{ZN} + L_{ZD}$		
L_D	Remineralization rate	0.16 day^{-1}
l_0	Remineralization rate at 0 °C	0.1 day^{-1}
w°	Proportional factor of sinking	1.2 m day^{-1} (mmol N)$^{-2}$ m^6
w_D	Sinking velocity of detritus	5.0 m day^{-1}
P_0	Background value for P	0.005 mmol N m^{-3}
Z_0	Background value for Z	0.005 mmol N m^{-3}

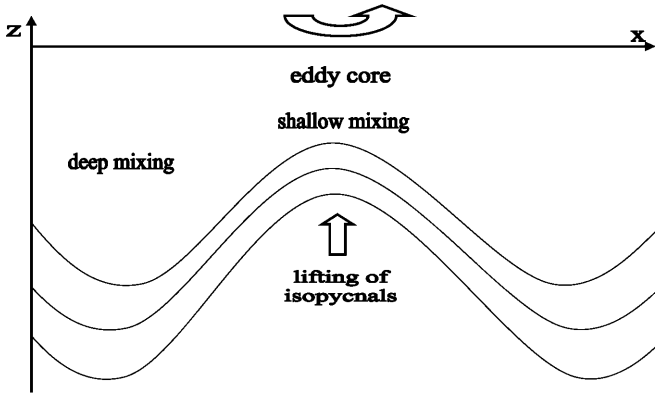

Fig. 2 Schematic circulation of a cyclonic eddy. The isopycnals are lifted in the center and vertical mixing is reduced there

concentration is 5 mmol N m^{-3} which is the typical nitrate concentration in the western Baltic Sea in late winter (Nehring et al. 1995, 1996; Matthäus et al. 1997). A low initial phytoplankton concentration of 0.5 mmol N m^{-3} is assumed. This value corresponds to a chlorophyll concentration of 0.8 mg m^{-3}, using the Redfield ratio (C:N = 106:16) and a carbon to chlorophyll ratio of 50. The initial values for zooplankton and detritus are 0.5 mmol N m^{-3} and 0.05 mmol N m^{-3}, respectively. The simulation starts at March 15, since the spring bloom usually commences in March in the Arkona Sea (Kaiser and Schulz 1978).

2.3 A three-dimensional physical/biological model

The three-dimensional physical/biological model was described earlier by K. Fennel (1999). It consists of the modular circulation model MOM1 (Pacanowski et al. 1990) and the biological model described above. The biological model differs slightly from the above description by the inclusion of temperature-dependent growth and respiration rates of phytoplankton and a temperature-dependent remineralization rate of detritus. These modifications have been found to be important for simulations running over a yearly cycle, but do not affect the results presented in this study and are given only for the sake of a complete description. Employing the Q_{10} concept of Eppley (1972), the rates read

$$w_{\max}(I,N,T) = w_{\max_0}\exp(aT)\frac{N^2}{k_N+N^2}\frac{I}{I_{\text{opt}}}\exp\left(1-\frac{I}{I_{\text{opt}}}\right) , \quad (9)$$

$$L_{PN}(T) = e_0\exp(aT) \text{ and} \quad (10)$$

$$L_D(T) = l_0\exp(aT) , \quad (11)$$

where $w_{\max_0}$, e_0, and l_0 represent the maximum growth, respiration, and remineralization rates at 0 °C. Since temperatures vary by less than 0.2 °C within the spatial and temporal range considered here, the temperature dependence does not affect the results and is neglected in the process-oriented model. The parameters in the process-oriented model are chosen to be consistent with the corresponding temperature-dependent parameters in the three-dimensional model.

The biological model is incorporated into the circulation model by means of advection-diffusion equations for the state variables which are treated as non-conservative tracers. Tracer advection is modeled using central differences in space and time. This advection scheme is conceptually simple, second-order accurate, and introduces little implicit diffusion, but is not positive definite; that is, advection of steep gradients in tracer distributions can lead to numerical overshooting and unrealistic negative concentrations of the biochemical variables. However, due to the high spatial resolution and the small integration timestep of the three-dimensional model numerical overshooting did not occur.

A large-scale map of the western Baltic Sea including the model area is given in Fig. 3. In order to resolve the mesoscale circulation features, a small horizontal resolution of 1 nautical mile is employed in the model. The vertical spacing is 2 m for the uppermost 12 layers, gradually increasing for the deeper layers to a total of 22 layers. The model topography is shown in Fig. 4. The external forcing comprises daily averages of realistic wind, cloud cover, and air temperature observed at the weather station Arkona and the mast station of the Baltic Sea Research Institute at the Darss sill (see Fig. 4 for the locations of the stations). The wind forcing acts uniformly over the model area, and air temperature and cloudiness were kept homogeneous over the area as well. The initial conditions for temperature and salinity are three-dimensional distributions interpolated from climatological data. The vertical mixing coefficients are determined using the Richardson number model of Pacanowski and Philander (1981) while the horizontal turbulent viscosities and diffusivities are constant. The Richardson number–dependent parameterization for the vertical mixing takes into account stratification and vertical current shear. For large Richardson numbers, corresponding to low current shear, the vertical mixing is reduced. The net heat flux, represented by the downward flux of solar radiation reduced by the net upward flux of longwave back radiation, sensible heat, and latent heat, is parameterized following Rosati and Miyakoda (1988). The parameter values of the physical model are listed in Table 2. The three-dimensional simulations start on March 1, 1995.

3 Model results

3.1 Results and sensitivity of the process-oriented model

The process-oriented model was integrated for 20 days, starting March 15, with homogeneous initial distributions of the biological variables. Within 2 days of model integration horizontal gradients build up. At day 3 a maximum chlorophyll concentration of 1.4 mg m^{-3} in

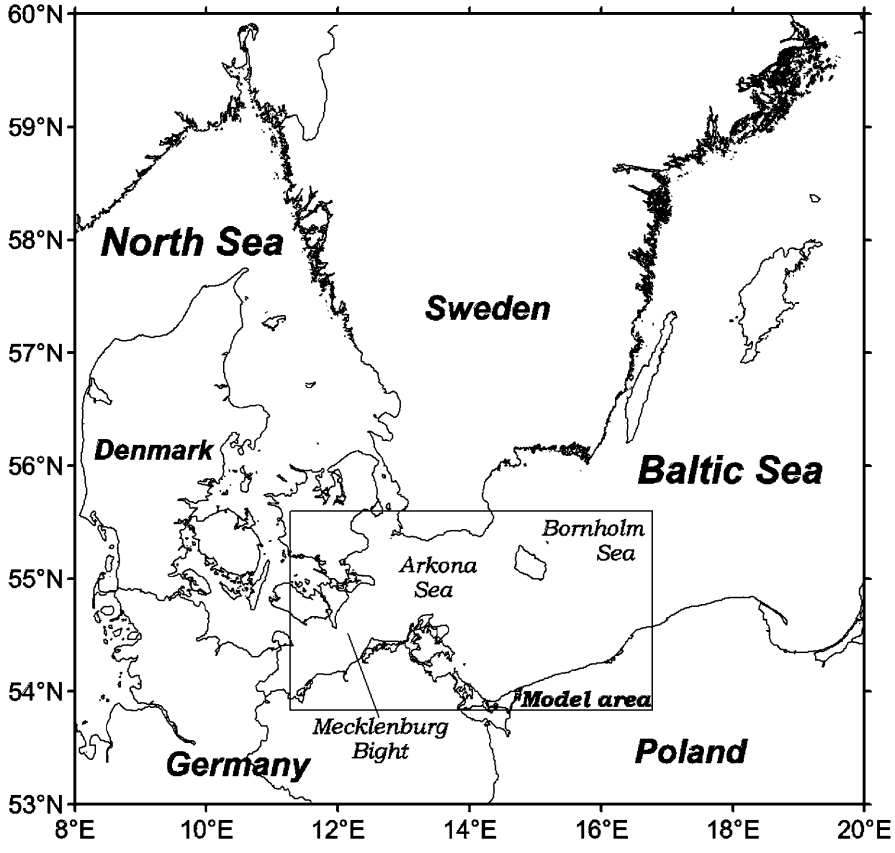

Fig. 3 Map of the western Baltic Sea. The model area is indicated

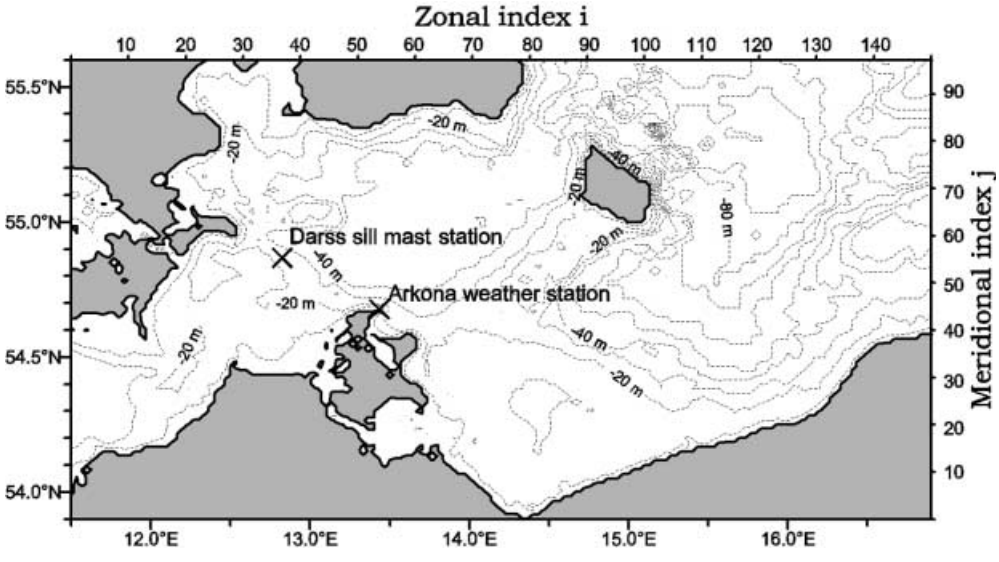

Fig. 4 Model topography including the locations of the measurement stations. At the *upper and right axes* the latitudinal and longitudinal model indices are indicated. The *horizontal grid width* is 1 nautical mile

the shallow mixed core compares to a minimum concentration of 0.9 mg m^{-3} in the deeper mixed regions. The magnitude of this concentration gradient increases rapidly. At day 6 there is a difference of 1.4 mg m^{-3} between the maximum concentration of 2.4 mg m^{-3} in the core and the minimum concentration of 1.0 mg m^{-3} in the deeper mixed region. By day 13 the difference increases to 4.2 mg m^{-3} between the values of 5.2 mg m^{-3} and 1.2 mg m^{-3} in the core and in the deeper mixed region (Fig. 5). Since phytoplankton growth is the dominant flux in both mixing environments and the magnitude of the growth rate is critically dependent on the mixing depth, the emergence of the concentration gradient is caused by the variations in mixing depth.

The dominance of the growth flux is illustrated in Fig. 6, where the course of the growth and loss terms is plotted for a shallow and a deeper mixed model location

Table 2 Parameter values of the circulation model

Symbol	Definition	Value
Δt	Time step	120 s
A_{hm}	Horizontal viscosity	10^5 cm^2 s^{-1}
A_{ht}	Horizontal diffusivity	10^5 cm^2 s^{-1}
A_{vm}	Vertical viscosity	0.0134–50 cm^2 s^{-1}
A_{vt}	Vertical diffusivity	0.00134–50 cm^2 s^{-1}
τ_b	Bottom friction	0.0025 dyn cm^{-2}
k_0	Extinction due to water	0.15 m^{-1}
k_1	Extinction due to chlorophyll	0.03 m^{-1} (mg chl m^{-3})$^{-1}$

(cf. Fig. 5). At both sites growth and respiratory losses of phytoplankton are the dominant fluxes during the entire integration period. Phytoplankton losses due to grazing, sinking, and mortality are much smaller. At site B the magnitude of the growth flux increases quickly with a doubled flux of 5 mmol N m^{-2} day^{-1} at day 6 compared with a value of 2.5 mmol N m^{-2} day^{-1} at day 1. After 10 days the growth flux has reached a magnitude of 8.2 mmol N m^{-2} day^{-1} – more than three times the value at day 1. At site A the growth flux also increases over time, but at a much lower rate. After 10 days the growth flux is still smaller than 3 mmol N m^{-2} day^{-1}. The respiratory losses also increase in time due to the higher phytoplankton standing stocks.

During the light-limited phase of the bloom, the phytoplankton growth rate is mainly influenced by the depth of the mixed layer. Variations in nutrient supply can be ruled out as a reason for the differences in the growth rate. Firstly, the nutrient distribution is initially homogeneous, thus another factor must account for the generation of the horizontal differences. Secondly, during the first 11 days of model integration, the nutrient concentrations lie in the saturation range of the growth response. The nutrient concentrations do not drop below 2 mmol N m^{-3} until day 11; that is, the nutrient supply supports maximum growth rates on the whole slab. To support this argument I calculated the explicit contributions of the nutrient-limited factor $f_1 = N^2/k_N + N^2$ and the light-limited factor $f_2 = \frac{I}{I_{\text{opt}}}\exp(1 - \frac{I}{I_{\text{opt}}})$ to the growth rate at the sites A and B. The mixed layer mean of the nutrient-limited fraction of the growth rate, f_1, over the first 10 days of the model integration differs negligible by a factor of 1.01 between site A and site B. The mixed layer mean of the light-limited factor, f_2, over the same period is twice as high in the eddy core at site B as at site A. Consequently the light supply is the most important factor influencing the growth rate during the first 2 weeks. The amount of light received by the phytoplankton population depends on the incoming radiation and the mixing depth. Since the incoming radiation does not vary horizontally, the variation in mixing depth must be crucial for the differences in phytoplankton growth.

The magnitude of the horizontal chlorophyll gradient varies over time as shown in Fig. 7b. It increases during the first 12 days when phytoplankton growth is the dominant process. The concentration gradient decreases again during the following days as nutrient availability starts to limit phytoplankton growth at site B and respiratory losses become more important there. The course and magnitude of the horizontal concentration gradient does not depend critically on the particular choice of the light response of phytoplankton, the starting date of the simulation, or the magnitude of the minimum and maximum mixing depths. A comparison with the results of three modified model runs illustrates this (Fig. 7). The light response was altered by employing another widely used parameterization for the photosynthetically active radiation (see e.g., Cullen 1990)

$$f(I) = P^B_{\max}[1 - \exp(-\alpha I/P^B_{\max})] \ , \tag{12}$$

where $P^B_{\max}$ and α represent the maximum rate of photosynthesis and the initial slope of the response, respectively. The formulation of the phytoplankton growth rate changes from Eq. (1) to

$$w(N, I) = w_{\max}\frac{N^2}{k_N + N^2} f(I) \ . \tag{13}$$

This modification leads to a slightly stronger response. The maximum concentration gradient between sites A and B is reached 4 days earlier and is a little larger than in the standard simulation (Fig. 7). Changing the starting date of the model run from March 15 to April 1 also shifts the model response slightly (Fig. 7). An increase of the maximum mixing depth by 5 m delays the

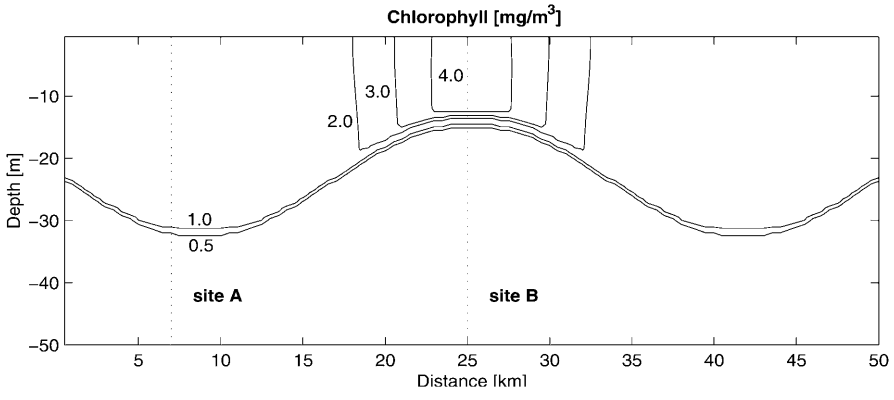

Fig. 5 Chlorophyll concentrations simulated by the process-oriented model after 10 days of model integration

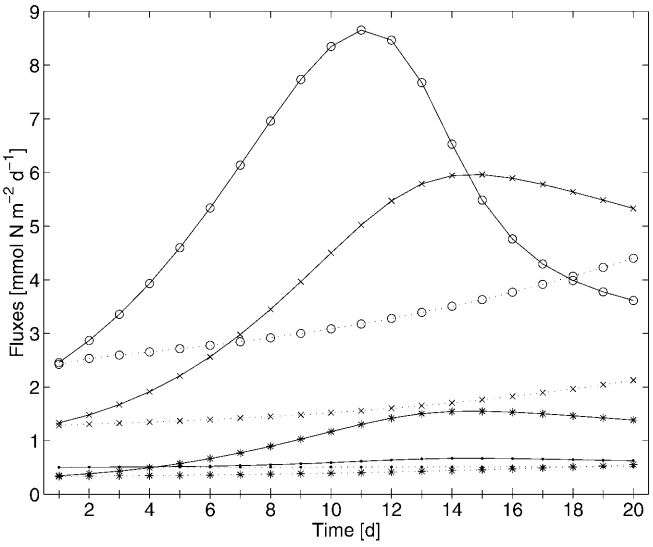

Fig. 6 Course of the phytoplankton source and sink terms integrated over the uppermost 40 m of the water column. *Dotted lines* refer to site A and *solid lines* to site B corresponding to the eddy center (cf. Fig. 5). Phytoplankton growth (○) and respiration (×) are the dominant fluxes, while grazing (·), mortality (∗), and sinking (+) are of only minor importance

occurrence of the maximum concentration gradient by 3 days (Fig. 7).

3.2 A three-dimensional simulation

A run of the coupled physical/biological model was performed for spring 1995 to simulate nutrient and plankton distributions during spring in the western Baltic Sea. The simulated current patterns are characterized by a high degree of mesoscale variability which evolves in response to the wind forcing and irregular bottom topography and coast lines. The initially homogeneous distributions of nutrients and phytoplankton reflect the physical variability and show considerable spatial variability already during early spring. A comparison of the simulated phytoplankton distribution with corresponding high-resolution chlorophyll measurements obtained during the Finnish phytoplankton monitoring project Algaline (see Rantajärvi and Leppänen 1994 for details) has been presented in K. Fennel (1999). Good agreement in spatial scale and amplitude of the chlorophyll variations has been shown between the simulated and observed distributions. The simulated chlorophyll on a longitudinal section was characterized by differences in concentration of 2 mg chl m^{-3} on a spatial scale of ~20 km. These variations compared well with the corresponding observed section (K. Fennel 1999). Since the model captures the observed mesoscale variability qualitatively, a study of the effect of flow patterns on phytoplankton patchiness is feasible.

In correspondence to the one-dimensional simulation presented above, the initial distributions of nutrients and plankton are homogeneous in the vertical and horizontal directions. Differential grazing or differential nutrient supply can be excluded as possible reasons for the generation of phytoplankton patchiness since zooplankton concentrations are as low as 0.5 mmol N m^{-3} and nutrients are sufficiently available with concentrations in the saturation range of the growth response. The generation of spatial gradients can be explained by differential growth rates induced by the proposed mechanism. A cyclonic eddy which occurred in the middle of March in the Arkona Sea (Fig. 8) serves as an example. Prior to its occurrence on March 14, nutrients and chlorophyll were distributed homogeneously in the Arkona Sea with chlorophyll concentrations of 1.3 mg chl m^{-3} and nitrate concentrations of 4.7 mg N m^{-3} (Fig. 9). From March 16 to 19 the cyclonic eddy was observed with a rotational flow field that extends from the surface to the bottom of the water column. The vertical mixing pattern connected with the eddy is shown in Fig. 10, the corresponding temperature and salinity sections are given in Fig. 11. I consider the area between the zonal indexes 68 and 74 and depth

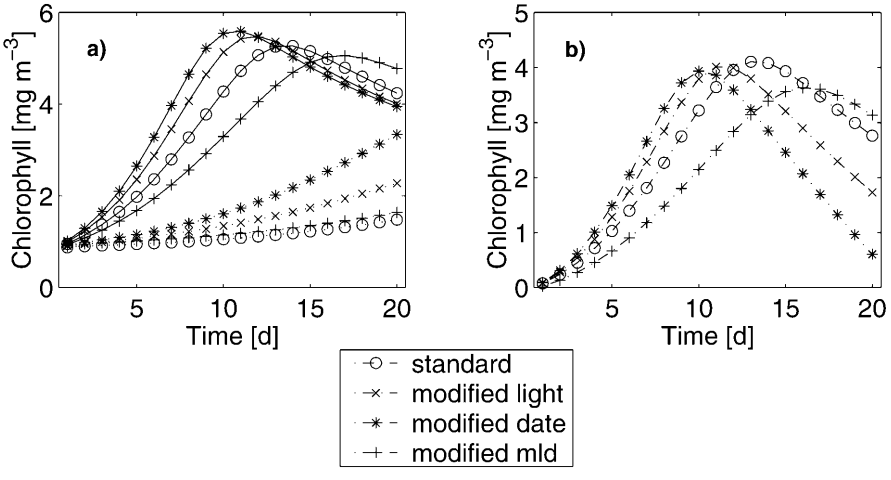

Fig. 7 a The simulated chlorophyll course of the standard model run (○) is compared with results of modified models at site B (*solid line*) and site A (*dotted line*). **b** Difference in the chlorophyll concentrations between both sites

index 8 (16 m) as eddy core, based on the hydrographical properties (salinity < 8 PSU and temperature < 2.8 °C in Fig. 11). The mixing coefficients are substantially reduced in the core, while mixing is maximal in the eddy ring (Fig. 10). This corresponds qualitatively to the pattern assumed for the process-oriented model described above. The sections of salinity and temperature show a slightly lower salinity and higher temperature in the core due to the reduced mixing (Fig. 11). The reduced vertical mixing in the eddy core supports higher growth rates of phytoplankton. Within 3 days (March 14 to March 16) the chlorophyll concentrations clearly increase in the core to 1.6 mg chl m^{-3}, exceeding concentrations in the surrounding environment by 0.2–0.4 mg chl m^{-3} (Fig. 9 and Figs. 12 to 14). The eddy declines during the following days.

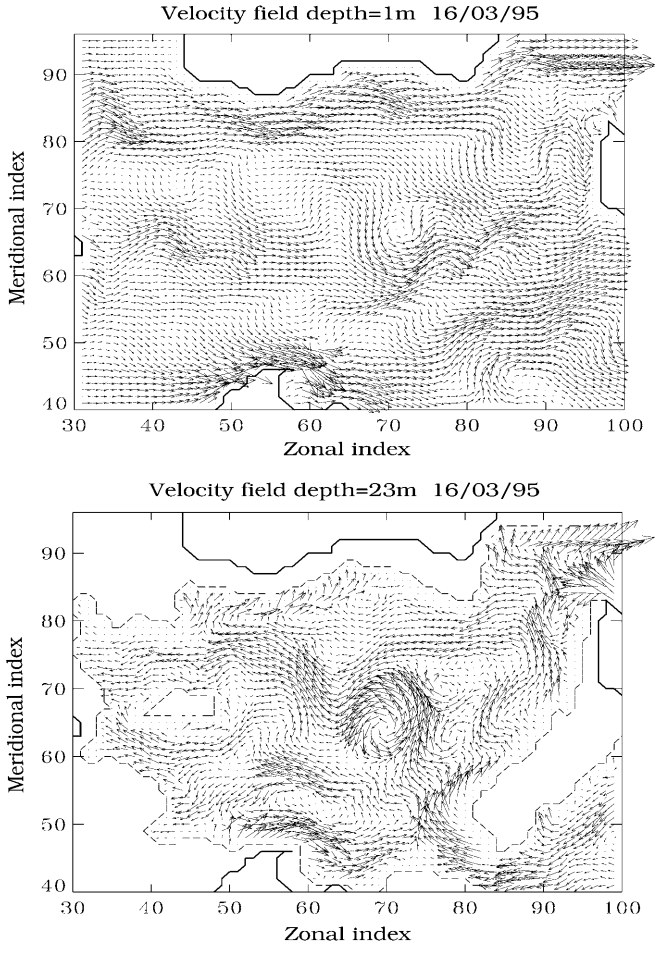

Fig. 8 The simulated current field in the Arkona Sea on March 16 in the uppermost model layer (*upper panel*) and at 23 m depth (*lower panel*). A cyclonic eddy is visible between the zonal and longitudinal indices 60 to 80. The horizontal extension of the eddy is approximately 10 nautical miles. The center of the eddy is located between the zonal indices 70 and 75 at the surface (*upper panel*) and at the zonal index 70 at the bottom (*lower panel*). The slight discrepancy in zonal direction between the surface and bottom location is due to the tilting of the rotation axis of the eddy caused by the eastward mean flow of the velocity field

In the western Baltic Sea, mesoscale flow patterns like eddies are of transient nature, with time scales typically ranging from a couple of hours to a few days. The flow field is usually characterized by a superposition of mesoscale patterns, including eddies, rather than the occurrence of single distinguished eddies. After a wind event, the mixed layer depth will initially reflect the generated eddy structure with a smaller mixing depth above cyclonic and a larger mixing depth above anticyclonic eddies, but horizontal advection will make the relation between mixed-layer depth and eddy field more complex over time. Klein and Hua (1990) observed a cascade of sea-surface temperature variability, generated by a wind-induced mesoscale eddy field, from small wavenumbers to large wavenumbers within a few days. The advective flow field is likely to affect the phytoplankton distribution as well, hence chlorophyll concentrations are not expected to be well correlated with the eddy field after more than a few days. However, the suggested mechanism is probably a major factor contributing to the initial generation of horizontal gradients, which are then further modified by the highly variable current field. The model results show that the occurrence of a transient eddy with a lifetime of 3 days is able to generate a notable concentration gradient.

4 Discussion

Two models of different complexity were used to investigate the effect of eddy dynamics on phytoplankton growth. The generation of patchiness by the specific circulation of a cyclonic eddy was simulated in a nutrient-replete environment with initially homogeneous distributions of nutrients and plankton. Both models predict higher growth rates in the core of the cyclonic eddy. Since the core is characterized by reduced vertical mixing, it provides more favorable growth conditions for the light-limited phytoplankton population. Because of the enhanced phytoplankton growth in the core, horizontal gradients emerge. In the process-oriented model the concentration difference between the eddy core and the surrounding environment is 0.45 mg chl m^{-3} after 3 days – slightly more pronounced than in the three-dimensional simulation, where a concentration difference between 0.2 and 0.4 mg chl m^{-3} is predicted after 3 days. The difference between the two models can be attributed to the idealized setup of the process-oriented model, which neglects advection and horizontal diffusion. According to the simulation, the local enhancement of growth by mesoscale current features, as postulated by Elken et al. (1994), can occur prior to the establishment of thermal stratification, which is generally considered a necessary condition for phytoplankton growth in the Baltic Sea in spring. The mechanism will apply during the light-limited phase of the bloom until nutrient limitation comes into play.

The described mechanism is based on the assumption that a shallow mixed layer is necessary to initiate a

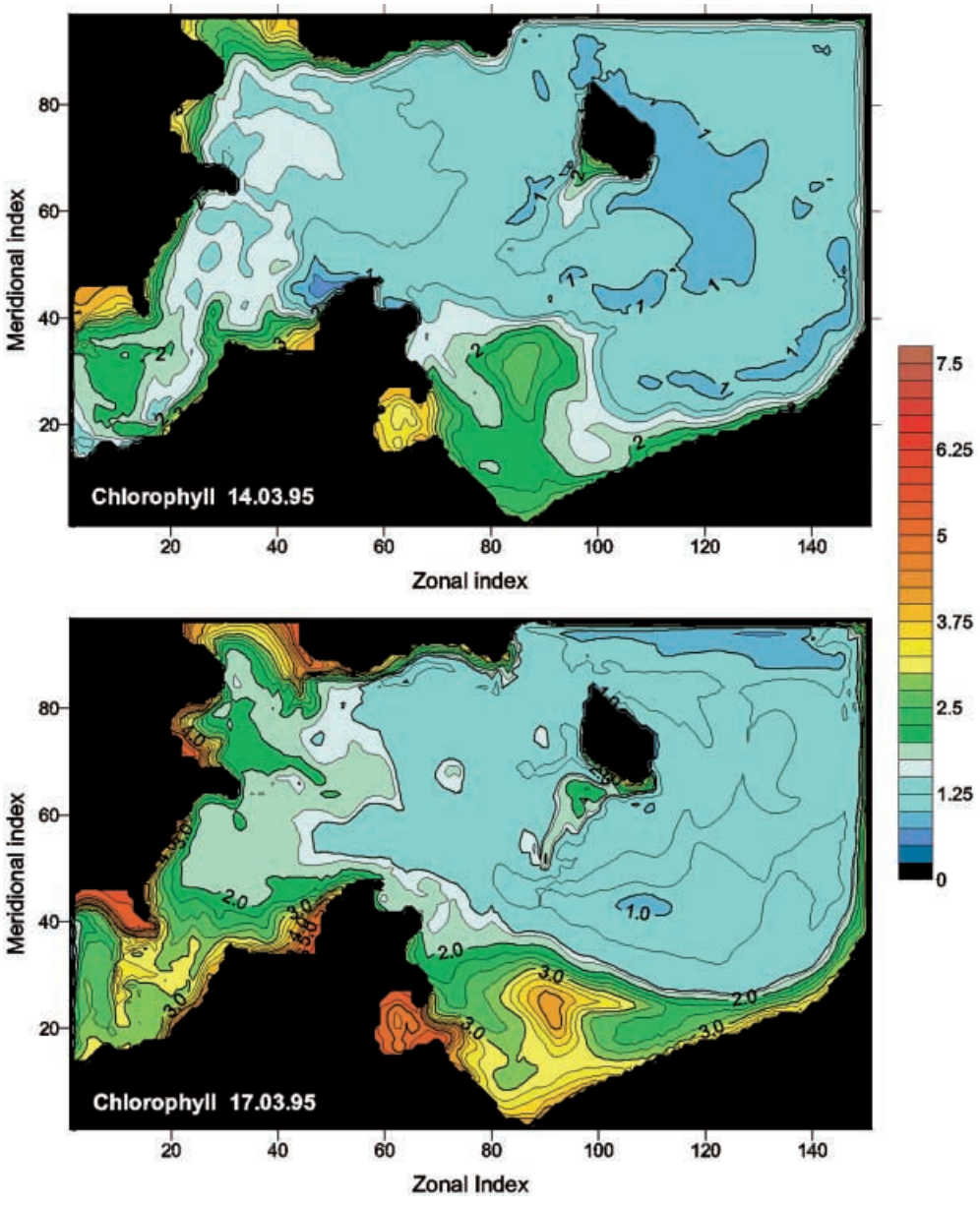

Fig. 9 Simulated phytoplankton distribution on March 14 (*upper panel*) and March 17 (*lower panel*). Chlorophyll concentrations in the uppermost model layer are plotted. A local maximum of chlorophyll is visible at the location of the eddy between the zonal indices 70 and 75 (*lower panel*, cf. Fig. 8)

phytoplankton bloom, according to the concept of Sverdrup (1953). Huisman et al. (1999) suggested an alternative mechanism for the generation of phytoplankton blooms, invoking a critical level of turbulence in contrast to the critical depth concept of Sverdrup. The authors postulated that a phytoplankton bloom can occur in weakly mixed environments without the existence of water-column stratification, if the vertical mixing is low and the phytoplankton growth rate exceeds the vertical mixing rate. This mechanism may be important in clear waters with weak vertical mixing (Huisman et al. 1999). The Baltic Sea in spring is characterized by intense wind mixing, and a relatively shallow upper mixed layer is necessary to initiate a phytoplankton bloom.

Previously suggested mechanisms like predator–prey interactions (Steele and Henderson 1992), diurnal vertical migrations of zooplankton (Mackas and Boyd 1979), or spatially varying vertical transport of nutrients into the euphotic zone (Aitsam 1994) do not serve as likely explanations for the generation of patchiness during nutrient-replete spring conditions. Although mesoscale transport patterns affect the distribution of plankton particles and may induce injections of nutrients into the euphotic zone, these physical transport mechanisms alone can only modify existing gradients. They cannot produce them from initially homogeneous distributions. In typical summer situations when the euphotic zone is nutrient-depleted, topographically induced upwelling may transport nutrients into the euphotic zone locally. This causes patchy distributions in summer, but does not explain the intense variability observed during spring conditions. In temperate latitudes prior to the spring bloom it is reasonable to as-

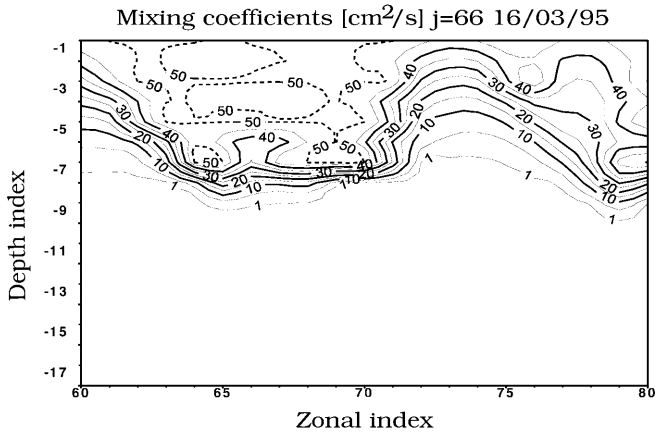

Fig. 10 Zonal section of the simulated vertical mixing coefficients at j = 66 (55°5′N) on March 16. The *depth index* refers to the layers of the model (the first 12 layers are 2 m thick). Vertical mixing is reduced in the core of the eddy between the zonal indices 70 to 75, whereas mixing is at maximum between the zonal indices 65 to 70

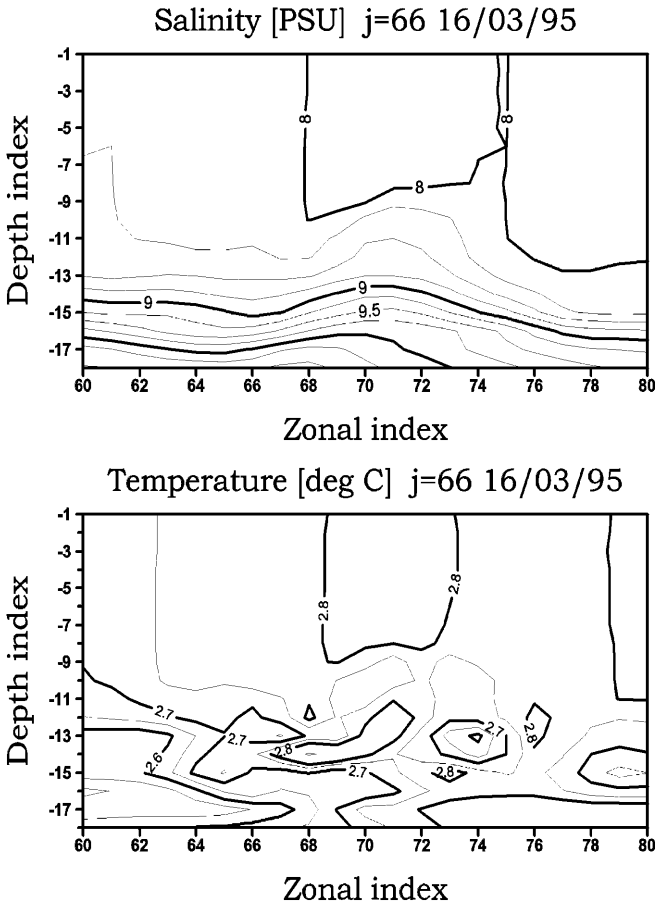

Fig. 11 Zonal section of the simulated salinity (*upper panel*) and temperature (*lower panel*) at j = 66 (55°5′N) on March 16

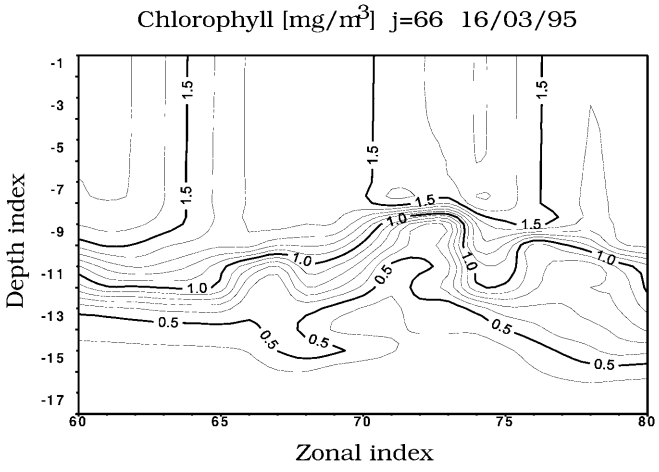

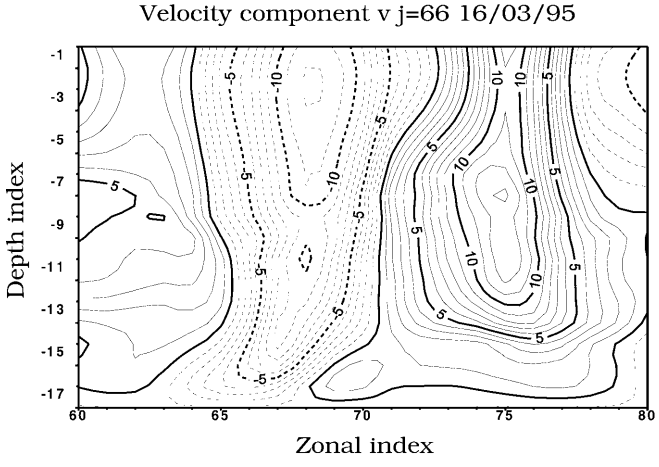

Fig. 12 Zonal sections of the simulated chlorophyll distribution (*upper panel*) and the velocity component *v* (*lower panel*) at j = 66 (55°5′N) on March 16. Velocity is given in cm s^{-1}, with *dashed lines* representing negative values. The eddy core is situated between the zonal indices 70 and 75

sume that growth conditions are uniform in terms of nutrient availability and initial plankton populations. In this case there are only two principal reasons for the emergence of plankton patches: (1) the particles are transported by a movement relative to the current into the patch (differential transport) or (2) they are produced in the patch by a biological process which acts with higher efficiency there than in the surrounding region (differential rates). Differential transport appears, for instance, due to sinking or floating of phytoplankton (Franks 1992, 1995, 1997), or diurnal vertical migration of zooplankton (Rovinsky et al. 1997). Differential rates occur when processes depend on nonisotropic conditions such as light or biochemical gradients. All these differential mechanisms arise from a nonlinear response to the current field.

An elevated growth in the core of mesoscale eddies was observed as early as 1941 in the area off the Southern California coast, where Sargent and Walker (1948) found an association of high diatom abundances with a cyclonic eddy. Mesoscale current patterns also affect phytoplankton growth patterns in the Southern Ocean (Strass et al. 1998; Moore et al. 1999), where productivity is generally low except at a narrow band associated with the Polar Front (PF) jet. The PF is

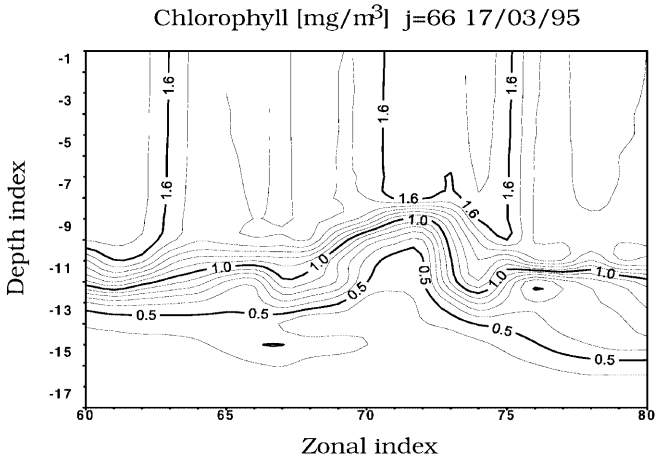

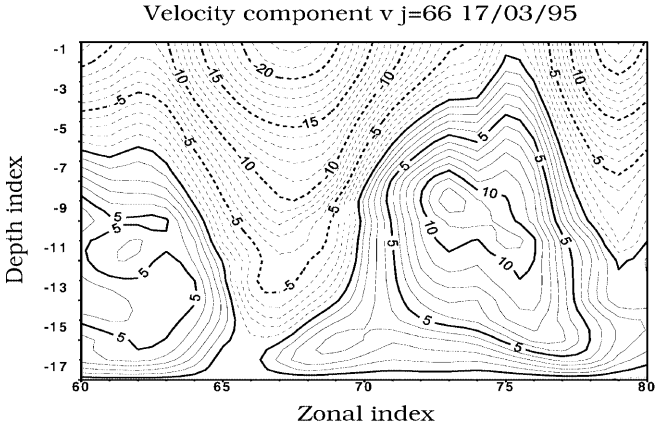

Fig. 13 Fig. 12 for March 17

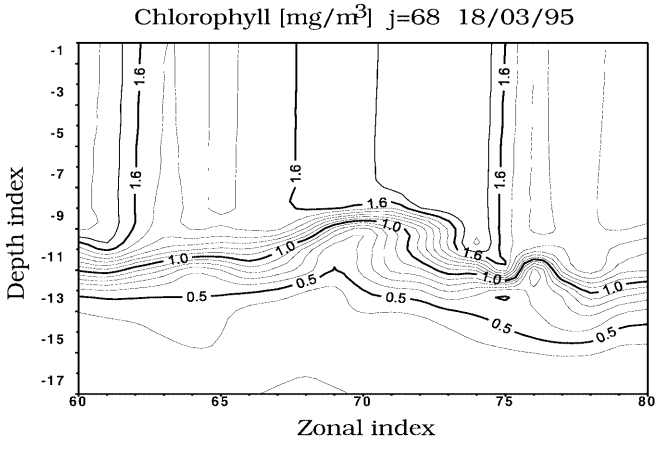

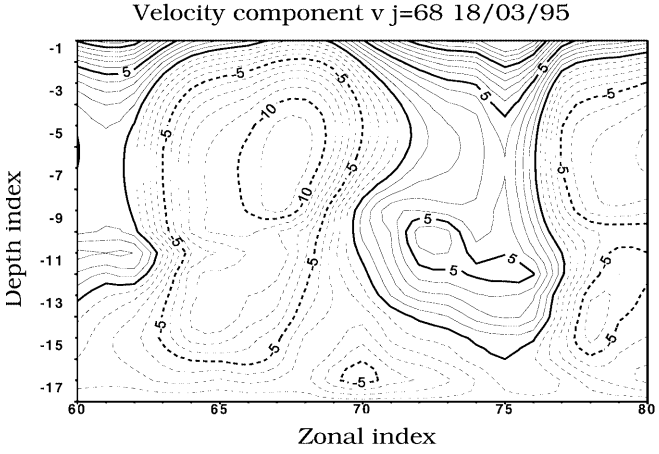

Fig. 14 Fig. 12 for March 18. An increased chlorophyll concentration associated with the eddy core is obvious. Note that this section has been taken at the meridional index 68 (55°7′N) instead of 66 (55°5′N) in Figs. 12 and 13. This cross-section has been shifted since the eddy moved northward since March 16

characterized by intense mesoscale variability which has been found most important for the distribution of biomass (Moore et al. 1999). Besides the possible iron limitation, phytoplankton growth is largely limited by light (Nelson and Smith 1991). Hence a local stabilization of the water column due to mesoscale features like meanders and eddies can create favorable light conditions. Consistent with the mechanism described in this paper, Barth et al. (2001) observed a localized high–chlorophyll patch associated with the cyclonic bend of a PF jet meander. Despite its relatively high advection velocities, this patch stayed in place with respect to the meander, implying a continuous growth at this location. An important influence of eddy dynamics on primary production patterns is also known from the Sargasso Sea in the North Atlantic, although a different mechanism is acting (Falkowski et al. 1991; McGillicuddy et al. 1998; Oschlies and Garçon 1998). The upper ocean layer in the Sargasso Sea is nutrient-depleted, so that an uplifting of the water column within the core of eddies results in an upward transport of nutrients. In this case, nutrient-rich water from below the nutricline is lifted into the euphotic zone and increases primary production.

5 Conclusions

The model results demonstrate that the nonlinear response of phytoplankton growth to the current field is a powerful mechanism for the generation of patchiness during nutrient-replete, light-limited growth conditions. During light-limited periods the characteristic circulation of eddies can produce differential growth rates (Elken et al. 1994). Due to the reduced mixing in the isolated core, the light supply is higher there, promoting locally elevated growth rates. In the Baltic Sea the mesoscale current field can favor phytoplankton growth prior to the establishment of the thermocline, which is generally regarded as the trigger for the phytoplankton spring bloom. The mechanism can be regarded as general and is likely to apply during light-limited periods in other regions that are characterized by mesoscale eddy variability as well, e.g., the frontal region of the Southern Ocean.

The effect of eddies on phytoplankton distributions leads to consequences for the spatial and temporal representativeness of in situ measurements. The actual current patterns should be taken into account when interpreting single samples. In the Baltic Sea the mesoscale current field can favor growth on small spatial scales prior to the establishment of the thermocline, which is generally regarded as the trigger for the phytoplankton spring bloom in that region.

Acknowledgements This work has been partially supported by a grant from the National Aeronautics and Space Administration (NAG5-4947). I am grateful to Richard Zeebe for helpful comments and encouragement and thank Bernadette Sloyan, Yvette Spitz, Jasmine Nahorniak, and Leon Tovey for their critical reviews of the manuscript. The thoughtful comments of two anonymous referees are greatly appreciated.

References

Abbott MR, Zion PM (1987) Spatial and temporal variability of phytoplankton pigments off Northern California during Coastal Ocean Dynamics Experiment 1. J Geophys Res 92C: 1745–1755

Abbott MR, Barksdale B (1995) Variability in upwelling systems as observed by satellite remote sensing: In: Summerhayes CP, Emeis KC, Angel MV, Smith RL, Zeitzschel B (eds.) Upwelling in the ocean: modern processes and ancient records. Wiley, New York, pp 221–238

Abraham ER (1998) The generation of plankton patchiness by turbulent stirring. Nature 391: 577–580

Aitsam A (1994) Physical and biological background of plankton patchiness. ICES Coop Res Rep 201: 3–7

Barth JA, Cowles TJ, Pierce SD (2001) Mesoscale physical and bio-optical structure of the Antarctic Polar Front near 170°W during spring. J Geophys Res 106G: 13879–13902

Brock TD (1981) Calculating solar radiation for ecological studies. Ecol Modelling 14: 1–19

Cullen JJ (1990) On models of growth and photosynthesis in phytoplankton. Deep-Sea Res 37: 667–683

Davis CS, Gallager SM, Solow AR (1992) Microaggregations of oceanic plankton observed by video microscopy. Science 257: 230–232

Denman KL, Platt T (1976) The variance spectrum of phytoplankton in a turbulent ocean. J Mar Res 34: 593–601

Elken J, Talsepp L, Kotus T, Pajuste M (1994) The role of mesoscale eddies and saline stratification in the generation of spring bloom heterogeneity in the southeastern Gotland Basin: an example from PEX'86. ICES Coop Res Rep 201: 40–48

Eppley RW (1972) Temperature and phytoplankton growth in the sea. Fish Bull 70: 1063–1085

Falkowski GP, Ziemann D, Kolber Z, Bienfang PK (1991) Role of eddy pumping in enhancing primary production in the ocean. Nature 352: 55–58

Fennel K (1999) Interannual and regional variability of biological variables in a coupled 3-D model of the western Baltic. Hydrobiologia 393: 25–33

Fennel W (1995) A model of the yearly cycle of nutrients and plankton in the Baltic Sea. J Mar Syst 6: 313–329

Franks PJS (1992) Sink or swim: accumulation of biomass at fronts. Mar Ecol Prog Ser 82: 1–12

Franks PJS (1995) Thin layers of phytoplankton: a model of formation by near-inertial wave shear. Deep-Sea Res 42: 75–91

Franks PJS (1997) Spatial patterns in dense algal blooms. Limnol Oceanogr 42: 1297–1305

Gower JFR, Denman KL, Holyer RJ (1980) Phytoplankton patchiness indicates the fluctuation spectrum of mesoscale oceanic structure. Nature 288: 157–159

HELCOM (1996) Third periodic assessment of the state of the marine environment of the Baltic Sea, 1989–93. Background document. Baltic Sea Environment Proceedings 64B, Helsinki Commission 1996, 252 pp

Huisman J, van Oostveen P, Weissing FJ (1999) Critical depth and critical turbulence: two different mechanisms for the development of phytoplankton blooms. Limnol Oceanogr 44: 1781–1787

Kaiser W, Schulz S (1978) On the causes of the differences in space and time of the commencement of the phytoplankton bloom in the Baltic. Kieler Meeresforsch Suppl 4: 161–170

Klein P, Hua BL (1990) The mesoscale variability of the sea surface temperature: an analytical and numerical model. J Mar Sys 48: 729–763

Kononen K, Nommann S, Hansen G, Hansen R, Breuel G, Gupalo E (1992) Spatial heterogeneity and dynamics of vernal phytoplankton species in the Baltic Sea in April–May 1986. J Plank Res 14: 107–125

Levin SA, Segel LA (1976) Hypothesis for the origin of planktonic patchiness. Nature 259: 659

Mackas DL, Boyd CM (1979) Spectral analysis of zooplankton spatial heterogeneity. Science 204: 62–64

Mackas DL, Denman KL, Abbott MR (1985) Plankton patchiness: biology in the physical vernacular. Bull Mar Sci 37: 652–674

Malchow H (1994) Nonequilibrium structures in plankton dynamics. Ecol Modelling 75/76: 123–134

Matthäus W, Nehring D, Lass HU, Nausch G, Nagel K, Siegel H (1997) Hydrographisch-chemische Zustandseinschätzung der Ostsee 1996. Mar Sci Rep 24

McGillicuddy DJ, Robinson AR, Siegel DA, Jannasch HW, Johnson R, Dickey TD, McNeil J, Michaels AF, Knap AH (1998) Influence of mesoscale eddies on new production in the Sargasso Sea. Nature 394: 263–265

Moore JK, Abbott MR, Richman JG, Smith WO, Cowles TJ, Coale KH, Gardner WD, Barber RT (1999) SeaWiFS satellite ocean color data from the Southern Ocean. Geophys Res Lett 26: 1465–1468

Nehring D, Matthäus W, Lass HU, Nausch G, Nagel K (1995) Hydrographisch-chemische Zustandseinschätzung der Ostsee 1994. Mar Sci Rep 9: 1–71

Nehring D, Matthäus W, Lass HU, Nausch G, Nagel K (1996) Hydrographisch-chemische Zustandseinschätzung der Ostsee 1995. Mar Sci Rep 16

Nelson DM, Smith WO, Jr. (1991) Sverdrup revisited: critical depths, maximum chlorophyll levels, and the control of Southern Ocean productivity by the irradiance-mixing regime. Limnol Oceanogr 36: 1650–1661

Onken R (1990) The creation of reversed baroclinity and subsurface jets in oceanic eddies. J Phys Oceanogr 20: 786–791

Oschlies A, Garçon V (1998) Eddy-induced enhancement of primary production in a model of the North Atlantic Ocean. Nature 394: 266–269

Pacanowski RC, Philander SGH (1981) Parameterization of the vertical mixing in numerical models of the tropical ocean. J Phys Oceanogr 11: 1443–1451

Pacanowski RC, Dixon K, Rosati A (1990) The GFDL modular ocean model users' guide version 1.0. GFDL Tech Rep 2, Princeton Univ., Princeton

Powell TM, Okubo A (1994) Turbulence, diffusion and patchiness in the sea. Philos Trans Roy Soc, London (B) 343: 11–18

Rantajärvi E, Leppänen J-M (1994) Unattended algal monitoring on merchant ships in the Baltic Sea. TemaNord 546: 1–60

Rosati A, Miyakoda K (1988) A general circulation model for upper ocean simulation. J Phys Oceanogr 18: 1601–1626

Rovinsky AB, Adiwidjaja H, Yakhnin VZ, Menzinger M (1997) Patchiness and enhancement of productivity in plankton ecosystems due to differential advection of predator and prey. Oikos 78: 101–106

Sargent MC, Walker TJ (1948) Diatom populations associated with eddies off Southern California in 1941. J Mar Res 7: 490–505

Siegel H, Gerth M, Neumann T, Doerffer R (1999) Case studies on phytoplankton blooms in coastal and open waters of the Baltic

Sea using Coastal Zone Color Scanner data. Int J Remote Sensing 20: 1249–1264
Smith SD, Dobson FW (1984) The heat budget at Ocean Weather Station Bravo. Atmos–Ocean 22: 1–22
Smith CL, Richards KL, Fasham MJR (1996) The impact of mesoscale eddies on plankton dynamics in the upper ocean. Deep-Sea Res 43: 1807–1832
Solow AR, Steele JH (1995) Scales of plankton patchiness: biomass versus demography. J Plank Res 17: 1669–1677
Steele J (1962) Environmental control of photosynthesis in the sea. Limnol Oceanogr 7: 137–150
Steele JH, Henderson EW (1992) A simple model for plankton patchiness. J Plank Res 14: 1397–1403
Stigebrandt A, Wulff F (1987) A model for the nutrients and oxygen in the Baltic proper. J Mar Res 45: 729–759
Strass VH, Naveira Garabato AC, Pollard RT (1998) Enhancement of primary production at the Antarctic Polar Front by mesoscale dynamics. Transactions, American Geophysical Union, EOS 79
Sverdrup JHD (1953) On the conditions for the vernal blooming of phytoplankton. J Con Int Explor Mer 18: 287–295